Development of a new method for neutron spectra analysis based on a deep learning algorithm for the detection of illicit materials

Clement Besnard Vauterin, Valentin Blideanu, Benjamin Rapp

M&C 2023 - The International Conference on Mathematics and Computational Methods Applied to Nuclear Science and Engineering · Niagara Falls, Ontario, Canada · August 13 – 17, 2023

Development of a New Method for Neutron spectra Analysis based on a Deep Learning Algorithm for the Detection of Illicit Materials

C. Besnard-Vauterin[1], V. Blideanu[1], and B. Rapp[1]

[1]Université Paris-Saclay, CEA, List, Laboratoire National Henri Becquerel (LNE-LNHB) F91120, Palaiseau, France

clement.besnardvauterin@cea.fr, valentin.blideanu@cea.fr, benjamin.rapp@cea.fr

ABSTRACT

The global context and the growth in international trade is widely recognized as a boon for the trafficking of illicit materials. In the area of homeland security, the active interrogation approaches used have failed to provide an up and running technique for non-intrusive on-site inspections. Neutron-induced reactions rely on precise measurement of gamma spectra, which is generally very complex due to high level of background noise. Active photon interrogation methods have also been overlooked but only in the context of actinide detection using photofission reactions. This work describes the design of a novel method for the detection of illicit materials based on active photon interrogation associated to photo-neutron spectrometry. It is the first attempt to explore the principle of inducing photonuclear reactions on samples to determine the composition of light elements such as nitrogen, oxygen and carbon and therefore to extend the use of active photon interrogation for the detection of conventional explosives, narcotics and chemical weapons. The approach is based on a source of photons produced by an electron linear accelerator to induce photonuclear reactions on different materials, on the spectrometry of the photo-neutrons created, and on the implementation of a new digital analysis method based on a convolutional neural network to identify the elements present in an irradiated compound and to extract their neutron contributions from the total neutron spectra. The results of this work shows that the use of photon interrogation coupled with a neural network trained with Monte Carlo simulated spectra can be a reliable alternative to the existing active interrogation techniques. Our study therefore provides the foundation of a new way of identifying elements based on photo-neutron spectrometry produced by bremsstrahlung photons.

KEYWORDS: homeland security, neutron spectrometry, neural network, Monte Carlo simulation

1. INTRODUCTION

In the field of material detection by non-intrusive on-site inspection, the existing techniques can be divided into two families depending on the exploring particles used. Neutron-induced reactions can be used to detect illicit materials in containers (the so-called active neutron interrogation method), using in particular the associated particle technique (APT) [1, 2]. In this case, the

detection is based on the measurement of gamma radiation produced by neutron-induced reactions (namely inelastic scattering, capture). However, the precise measurement of gamma spectra is generally complex due to the experimental conditions, being often characterized by a high level of gamma background. In the case of the use of photons, the method is called active photon interrogation (API) and is currently used only for threats related to nuclear materials based on the actinide detection using photofission reactions and spectrometry of gammas emitted subsequent to the decay of radioactive fission fragments [3].

Our work extends the applicability of traditional API techniques by the development of a novel method allowing for the first time the detection of light elements (nitrogen, oxygen and carbon) present in illicit materials (conventional explosives, narcotics and chemical weapons) based on active photon interrogation associated to photo-neutron spectrometry. This new method overcomes the difficulties related to gamma-ray spectrometry on which the neutron interrogation is based [4]. In addition, compared to the active neutron interrogation method, it has the advantage that photons are much more penetrating than neutrons for most materials and therefore less subject to scattering and attenuation. The principle of the method involves inducing photonuclear reactions on these nuclei using ideally mono-energetic photons, with energies above threshold which is around 10 MeV for nitrogen isotopes. This leads to nuclear excitation and subsequent emission of neutrons. The measurement of their spectra allow the identification of the emitting nuclei and potentially to determine their quantity. The existence of energy levels in nuclei and, moreover, their low density for light nuclei gives to the energy spectra of the emitted photo-neutrons the particularity of presenting distinctive peaks at well-known energies.

Among the existing photon sources suitable for this purpose, compact single and dual energy sources with energies above 10 MeV can be obtained namely based on low-energy proton induced resonance reactions. These sources are however multi-directional with low effective photon intensities in a given solid angle thus significantly degrading the signal over noise ratio. Another approach, which avoids this limitation while being simpler to set up given the higher availability of the required equipment, consists of using a source of photons produced by an electron linear accelerator (LINAC). However, the bremsstrahlung photons produced in this way do not meet the conditions mentioned above relating to their energy spectrum, which is in this case continuous. Therefore, the implementation of this method requires a special treatment in order to select in the total spectrum of the detected neutrons generated in photonuclear reactions by all photon energies the events associated with a given energy of the photon. This approach, known as the "tagged photon" method, can be implemented experimentally by using additional equipment but this requires the deployment of a complex and non-compact system for electron spectroscopy and electron-neutron coincidence electronics.

Our new approach intends to overcome these limitations. The selection of contribution from photons in a well-defined energy range was achieved by subtracting two neutron spectra induced by bremsstrahlung photon beams created by electrons of close energies. Deep learning-based methods inspired by the chemometrics field [5, 6] were further used to recognize and identify the signatures of particular elements in compounds from simulated raw neutron spectra and to extract their respective contributions.

2. METHOD

The method presented in this paper for the identification of elements in a compound based on their neutron energy spectra after being irradiated by a bremsstrahlung photon source relies on convolutional networks that are trained with Monte-Carlo simulated data. The establishment of a sufficiently rich learning database is made possible by the ability of Monte Carlo simulation to generate a very large amount of data provided that the physics used is accurate enough and the computing power is sufficient. Such datasets would have been impossible to build by measurements. In order to dispose of reliable simulated neutron spectra that are consistent with physics and the law of energy conservation, a benchmark of four Monte-Carlo simulation codes was firstly performed. Then, simulations of pure element irradiation by 18 MV and 20 MV bremsstrahlung photon beams were performed with the selected Monte-Carlo N-Particle code MCNP6.2. Data augmentation was applied for each element in the database. One-element identification models were built using convolutional neural networks (CNN) [7] to predict the existence of each element in the compounds. All the one-element identification models were trained and stored for reload. A dataset of simulated neutron spectra of compound and a ternary mixture dataset were used to test the performance of the developed algorithm. The flowchart of the proposed deep learning-based neutron spectra identification (DeepNSI) is shown in Appendix A.

2.1. Monte-Carlo Codes Benchmark for Photo-neutron Energy Spectra

Training datasets for neural networks being based on Monte-Carlo simulated neutron spectra, the capabilities of the existing codes to accurately simulate the photonuclear reactions and a good understanding of physics involved become crucial. In that matter, the neutron energy spectra from photo-nuclear reactions at 20 MeV were calculated and the results compared using the main Monte-Carlo codes used by the community: FLUKA [8], GEANT4 [9], MCNP [10] and PHITS [11]. Considered materials were carbon and nitrogen as they are of interest for the detection of illicit materials.

As presented on Figure 1 the shape of the photo-neutrons spectra is strongly influenced by nuclear levels structure of light elements. Significant differences in how this effect is handled by the various codes are identified, with an extreme behavior in the case of PHITS for which physics models and data libraries available in the current distribution package do not account at all for this effect. Peak positions present in the simulated photo-neutron spectra have been carefully checked for both elements and found to be generally in coherence with the energy conservation of the reaction and nuclear energy levels of each nucleus. As there are no experimental neutron spectra to compare to the simulated ones, this energy conservation aspect is the only indicator available to check the consistency of the simulated spectra.

Special attention is given to the neutron spectrum from nitrogen irradiation as this element can be used as marker allowing to detect conventional explosives, narcotics and drugs and some chemical weapons with, notably, the emergence of new compounds related to opioid attacks. Here, natural nitrogen with 99.6 % of N-14 and 0.4 % of N-15 was used. The density was chosen to be of $\rho = 1\ g/cm^3$. Both N-14 and N-15 have very close neutron separation energies of respectively 10.55 MeV and 10.83 MeV.

Given the conservation of the energy of the reaction, the energy of the photo-neutron can be calculated for each of the excited energy levels of the ejected nucleus. For N-13 (from the $^{14}N(\gamma,n)^{13}N$ reaction), the ground state predicts a photo-neutron at 8.92 MeV and the first four excited levels: photo-neutrons at 6.58 MeV, 5.52 MeV, 5.48 MeV and 2.87 MeV respectively. Figure 1 shows that Geant4, MCNP and FLUKA can reproduce the peaks at the expected neutron energies for the ground state and the first three excited states of what is most probably N-13 nucleus considering the isotopic ratio of N-14 in the natural composition of nitrogen. Below 2.5 MeV, no clearly discernible structure is observed due to the increase in density of higher excited states.

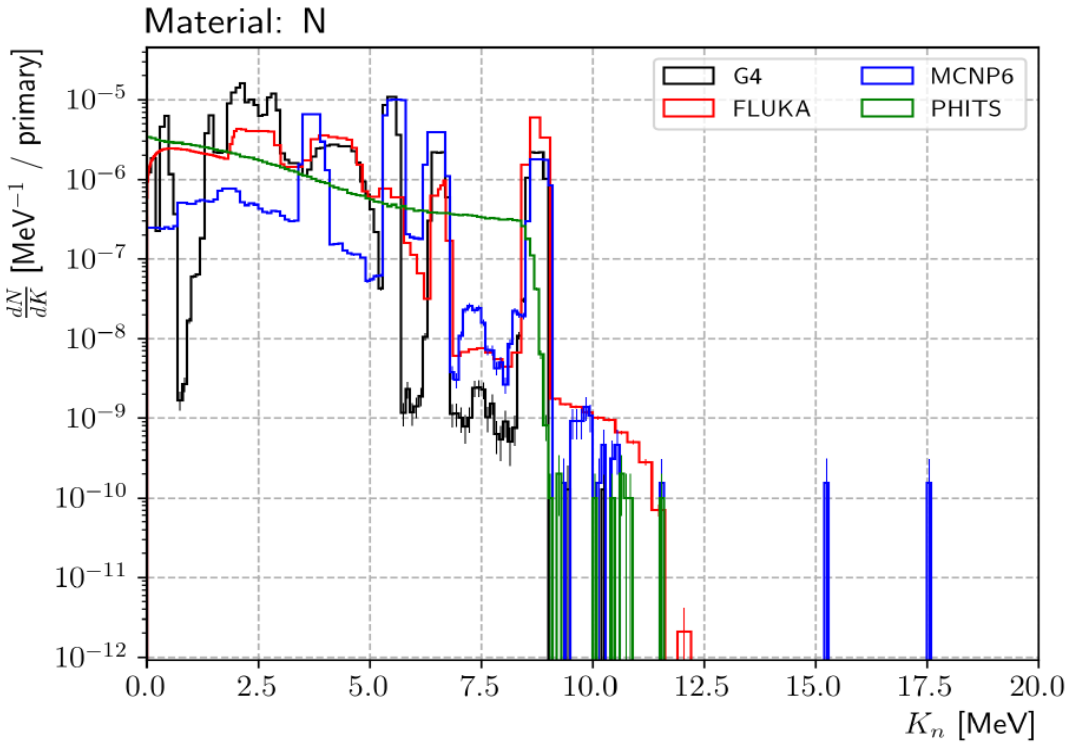

Figure 1. Photo-neutron energy spectra calculated using FLUKA, GEANT4, MCNP and PHITS for natural nitrogen with a 20 MeV monochromatic photon pencil beam.

Similar conclusions were drawn in the case of carbon. Based on the results of this comparison MCNP v6.2 has been selected to provide neutron spectra data to feed the training dataset as being a code more broadly used by the community and being able to provide reasonably reliable information given the above-mentioned considerations. Its capability to simulate the photonuclear physics was introduced in 2000 through tabular data sampling. The tabular data used here is known as the LA150 library [12].

It comprises a complete photonuclear evaluation in the ENDF-6 format for several elements. It was published under the '24u' library ID as the LA150u ACE library (see ref. [13]) and used for MCNP6 simulations as the default library for the photonuclear physics. As for the inputs, the main concern is that Monte Carlo sampling of tabular data is inherently limited by their availability. In the presented study, materials cards were specified using isotopic nuclei identifiers. For each of them, considered neutron and photonuclear transport data are taken form the only available LA150

library. The lack of a needed tables is normally handled by using physics models but this was not the case for the materials used in this study.

2.2. Neutron Energy Spectra Dataset and Data Augmentation for each Element

The database contains the simulated neutron spectra of 11 pure elements, which are common light elements situated in the first three rows of the periodic table. This database was established through simulations with the MCNP6.2 Monte-Carlo code. For each element, two neutron spectra are recorded in the database from simulations with two different bremsstrahlung photon beam energies (18 MV and 20 MV). These different bremsstrahlung photon beams were generated by simulating the interaction of two electron beams with Gaussian energy distributions centered at 18 MeV and 20 MeV respectively with a thin 10 µm thick pure gold target.

The neutron spectra were obtained using the simulation configuration consisting of a target (cylinder of 6 cm long and 4 cm diameter) irradiated by a 1 cm diameter parallel bremsstrahlung photon beam as discussed above. For each element the simulated neutron spectrum obtained with the 18 MV beam is subtracted from the one obtained with the 20 MV beam allowing the selection of the events corresponding to neutron emission from the reactions induced by photons with energies between 18 and 20 MeV. The spectra thus obtained show structures specific to each element and can be used as a particular signature for their presence in a compound material as shown on Figure 2. All spectra have been normalized to unity.

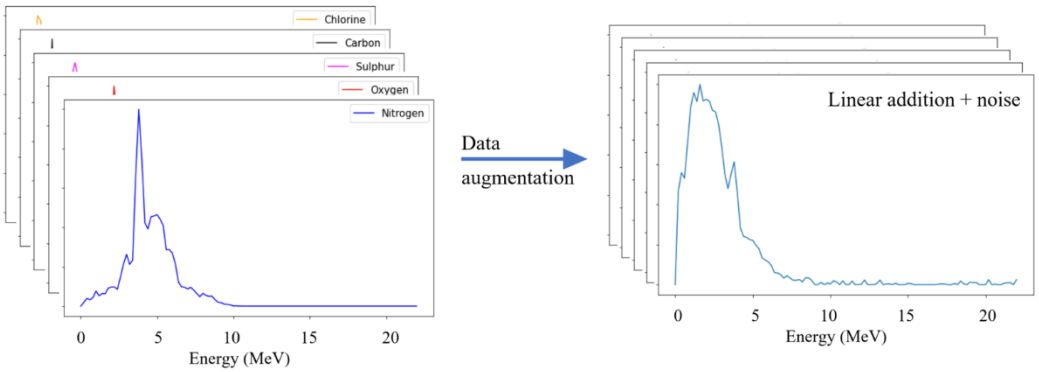

Figure 2. Samples of spectra from the irradiation of pure elements from the database used for data augmentation to build the training dataset.

Data augmentation was applied to solve the problem of the limited number of simulated neutron spectra used for training, validation and testing. For each element in the database, 20 000 artificially made mixture neutron spectra were randomly generated for both training and validation of its CNN models. 10 000 additional spectra were generated for both positive and negative configurations (respectively associated and not associated to a given element). For the positive neutron spectra, the ratios of the element were randomly generated in [0.1, 1.0], and the ratios of the other randomly chosen interference elements were randomly generated in [0.0, 1.0]. The negative spectra were generated by the superposition of other randomly chosen elements at random

ratios in the [0.0, 1.0] range. The obtained augmented dataset of each compound was divided into three parts: 15 000 as the training set, 2500 as the validation set, and 2500 as the test set.

2.3. Convolutional Neural Network for Element Identification

A CNN is a type of neural network that takes inspiration from biological processes. It is composed of convolutional and subsampling layers, with the option to add fully connected layers. The network typically consists of an input layer, a feature map layer, and a kernel function. The feature map is generated by sliding the kernel over the input with a set stride. Compared to a fully connected neural network (FCNN), a CNN benefits from shared weights, which improves learning efficiency and generalization, and sparse connectivity, which enables the network to respond strongly to local input patterns. CNN can extract spectral features and learn to recognize elements even amidst complex interferences. Since neutron spectra can be viewed as one-dimensional vectors, a four-layered one-dimensional CNN is used. The first two layers are convolutional layers; their number of convolution output dimensions is 32 and 64. They can extract the spectral features, while the last two layers are fully connected layers with 1024 and 2 nodes establishing the relationship between the feature maps and element presence. To enhance learning efficiency, a pooling function follows each convolutional layer. Dropout is employed between the fully connected layers to prevent overfitting. Rectified linear unit (ReLU) is used as the activation function between layers. The SoftMax function is applied to the final layer as it is commonly used for neural network-based classifiers. Its purpose is to normalize the predicted output, resulting in a probability distribution for the corresponding class. Each model of DeepNSI can be quickly reloaded for the prediction of elements or retrained and new ones can be easily added. Figure 3 represents the architecture of the CNN models used in DeepNSI.

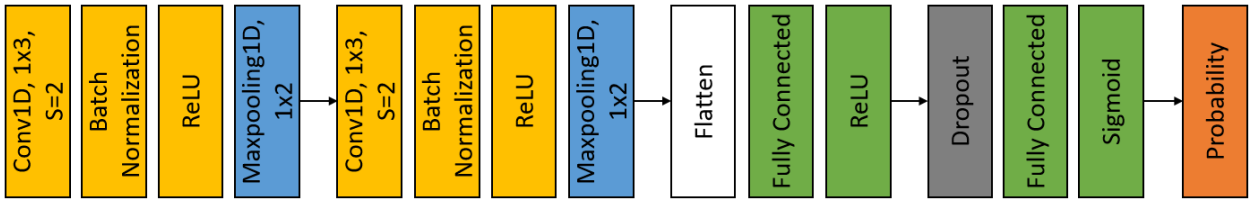

Figure 3. The architecture of the CNN model. A four-layer CNN model is used in DeepNSI.

The adaptive moment estimation [14] is used to train the networks since it requires little memory and has high computational efficiency. It is invariant to diagonal rescaling of the gradients and is well suited for problems that have a large amount of data. Cross entropy loss was used as the loss function. The weights of the network for kernels were initialized by truncated normal distribution. The learning rate was 5.10^{-5}, and the batch size was 512 after optimization. The epoch was in the range from 200 to 800 for models of different elements. The stopping criterion was if the increase of epoch had no obvious contribution to accuracy. The accuracy-epoch curve and loss-epoch curve are shown in Figure 4 (taking nitrogen and carbon as an example, while the other 9 models also achieve similar results).

Accuracy (ACC), true positive rate (FNR, sensitivity) and false positive rate (FPR, specificity) were used to evaluate the performance of the models for identification. The formulae for ACC, FNR and FPR are as follows:

$$ACC = \frac{TP+TN}{TP+TN+FP+FN}. \quad FNR = \frac{FN}{TP+FN}. \quad FPR = \frac{FP}{TN+FP}. \tag{3}$$

where TP, FP, TN, and FN represent true positive, false positive, true negative and false negative, respectively. For binary classification, the spectra during the training process were labelled either positive or negative.

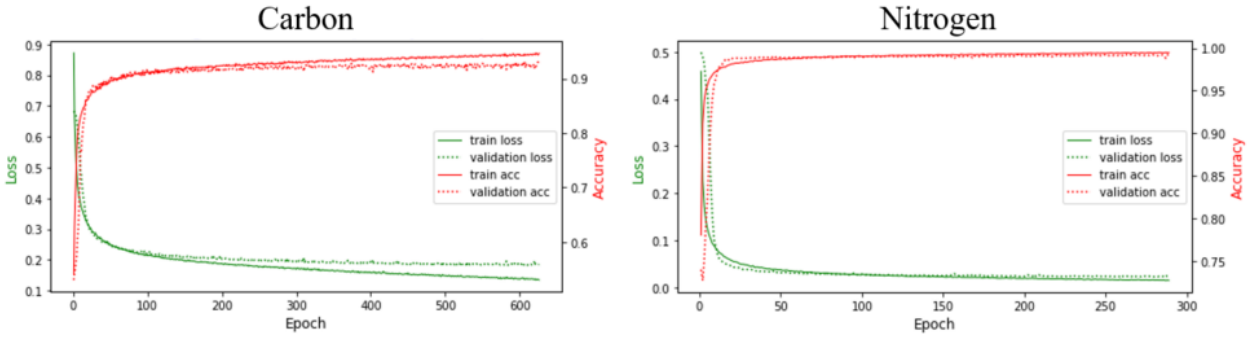

Figure 4. Accuracy-epoch and loss-epoch curves of a valid set during training (using carbon on the right and nitrogen on the left as examples).

2.4. Elastic Net Regularization for Contribution Estimation

Non-negative elastic net is used to determine the relative contribution of each element in the compounds. The method can be treated as a hybrid of lasso and ridge regression, which combines both the L1 and L2 regularization to improve the regularization of statistical models. Considering that the relative contribution of each element has to be non-negative, this restriction is imposed to ensure meaningful and valid results.

3. RESULTS AND DISCUSSIONS

3.1. Prediction Accuracy for Element Identification

Table I displays the outcomes of simulated data test sets for several elements. Amongst the 2500 simulated test samples for each element, DeepNSI exhibited significantly higher accuracy than k-nearest neighbor (k-NN) and support vector machine (SVM). Additionally, it outperformed random forest (RF) and gradient boosting decision tree (GBDT). DeepNSI showed comparable accuracy to logistic regression (LR) with L1-regularization for one-element identification models.

Table I. Prediction accuracy: Prediction accuracy (ACC) in percent of the element identification models on the simulated test sets by different methods. Only parts of the results are shown, concerning the elements of special interest for illicit material detection.

	DeepNSI	RF	GBDT	LR	k-NN	SVM
Carbon	97.9 %	89.8 %	95.4 %	97.5 %	87.9 %	84.7 %
Nitrogen	99.5 %	98.7 %	99.0 %	99.5 %	96.8 %	96.2 %
Oxygen	99.7 %	94.2 %	98.5 %	99.7 %	95.4 %	96.8 %
Chlorine	99.9 %	98.0 %	99.0 %	99.9 %	98.3 %	98.8 %
Sulfur	99.5 %	94.9 %	97.6 %	99.5 %	94.8 %	94.0 %

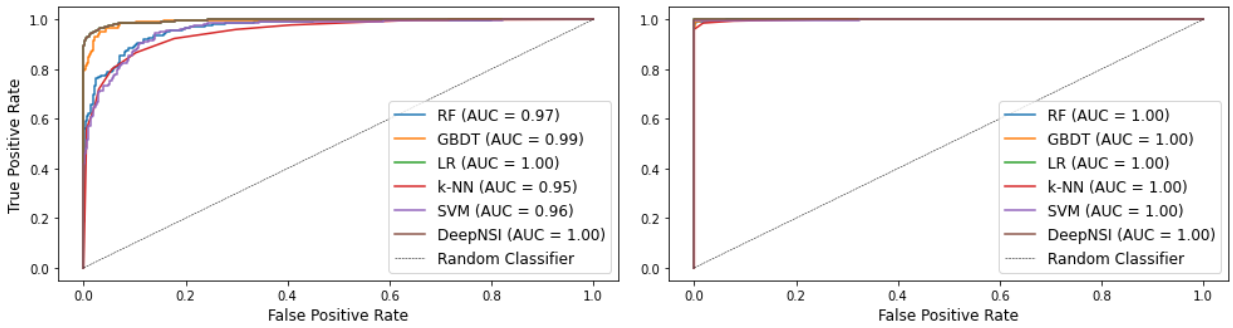

Figure 5. Receiver operating characteristic curves of the different machine learning methods for the prediction of carbon (on the left) and nitrogen (on the right).

Figure 5 demonstrates the receiver operating characteristic (ROC) curves for different methods, for carbon and nitrogen that were selected as examples because they yielded significantly different prediction accuracies. As evidenced by the ROC curves, DeepNSI's curve fully encompasses the curves of other methods. The ROC curve for LR with L1-regularization overlaid to that of DeepNSI, indicating that their performances surpass those of other methods. The ROC curves for carbon are somewhat worse than for nitrogen as the signature of this element is less distinct. C-11 (from the $^{12}C(\gamma,n)^{11}C$ reaction) emits only neutrons of about 1 MeV when excited by photons between 18 and 20 MeV. The neutron contribution of carbon is therefore often hidden by neutrons emitted by heavier elements such as aluminum or magnesium, which have in addition larger cross sections for photonuclear reactions.

3.2. DeepNSI on Artificially Made Compounds

Table II focuses on DeepNSI's performances using artificially made compounds, which are simply mixtures of neutron spectra of elements randomly selected from the database and added in random proportions. To each of these so produced spectra one can add a random noise on each energy bin varying between 0 and a certain percentage of the maximum of the concerned spectrum. The table below presents the details for only 6 of these spectra but a confusion matrix is available in Appendix B showing all the results for 1000 spectra of 3-element compounds and 1% noise. From

these figures it can be seen that, as intuitively expected, the prediction accuracy of DeepNSI decreases with increasing noise added to the spectra and with the number of elements added to the mixture, while remaining within acceptable limits for our purpose. This is due to the fact that each DeepNSI model has been trained on mixtures of 3 elements while being still able to make predictions on mixtures with more elements. In contrast to this trend, the false positive and false negative rates are increased by the noise.

Table II. Results of element identification: Results of element identification on artificially made compounds. The prediction accuracy as well as the false positive and false negative rates from DeepNSI's predictions are shown.

Runs	Elements in the mix	Noise	ACC	FPR	FNR
1	3	0 %	95.03 %	0.11 %	4.97 %
2	3	1 %	93.64 %	12.06 %	5.63 %
3	3	5 %	80.25 %	38.49 %	13.15 %
4	5	0 %	87.14 %	0.00 %	12.86 %
5	5	1 %	88.34 %	7.25 %	10.91 %
6	5	5 %	76.86 %	27.97 %	17.80 %

3.3. Prediction Result on a Monte-Carlo Simulated Compound Spectra Dataset

In this section, the prediction results from DeepNSI on Monte-Carlo simulated neutron spectra from various compounds of interest is discussed. Figure 6 is highlighting some of the results obtained. Overall, DeepNSI systematically finds the nitrogen and oxygen in the different molecules but not carbon when it is below 20% in atom fraction as the photonuclear reaction cross section for this element is very low (below 1 mb for photons in the 18 MeV – 20 MeV range). In addition, carbon spectrum is characterized by neutrons with energies around 1 MeV which are difficult to identify considering that more other neutron contributions are present in this energy region (emission for heavier elements present in the compound and originally energetic neutrons slowed down in the matrix).

The calculated contributions from each element in the compound's spectra does not correlate with the normalized atom fractions because of the differences in photonuclear reaction cross sections for the corresponding nuclei. This aspect has not been accounted for in this first estimate, intended mainly to demonstrate the appropriate performance achieved by the method proposed with respect to the accuracy in specifying the nature of compounds and differencing between explosives, chemical weapons, and narcotics.

The ternary plot on the right of Figure 6 was constructed on the basis of the neutron contributions estimated using non-negative elastic net and with the reference spectra of the elements in presence predicted by DeepNSI. In cases where carbon was not identified (such as for some explosives) or where the sum of the relative contributions of the three elements was different from 1, the complementary normalization to 1 on the three elements was added to the "carbon + other"

category without changing the estimated relative oxygen and nitrogen contributions. From this plot, two clusters are clearly identified, allowing the identification of the explosive and narcotic families. The neutron response of an unknown molecule can thus allow its classification based on the proximity to one of these clusters.

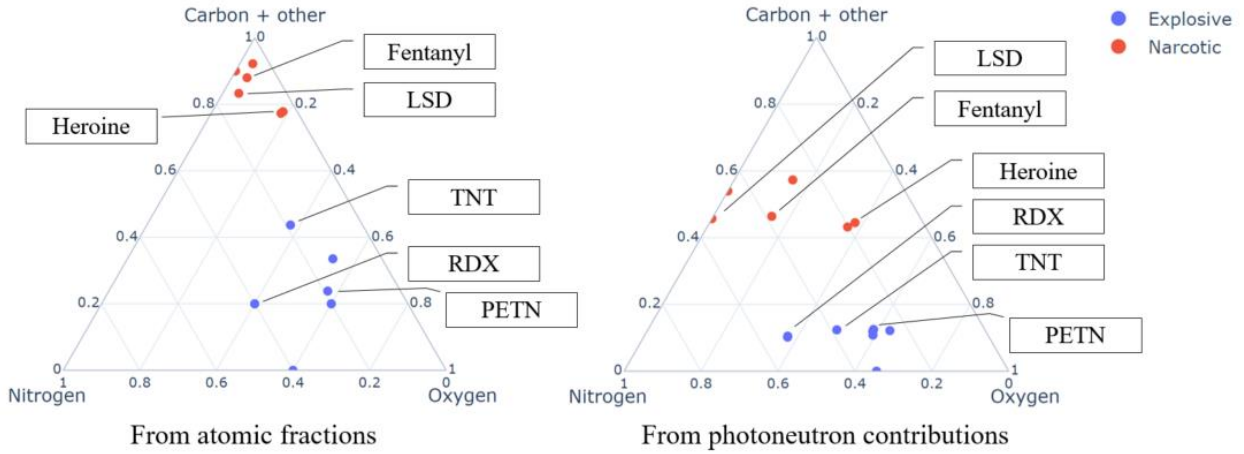

Figure 6. Ternary plots for several molecules of interest based on their carbon, nitrogen and oxygen ratios built upon the atomic fractions (left) and built upon the neutron contributions in the total neutron spectrum of each molecule (right).

4. CONCLUSIONS AND PERSPECTIVES

In this study, DeepNSI models were developed for element identification from photo-neutrons spectra emitted by bremsstrahlung photon-induced reactions based on deep learning techniques to be used in applications involving illicit material detection. Simulated datasets were used for the training and to evaluate its performances. The results show that DeepNSI can achieve better accuracy compared to other machine learning methods such as LR, kNN, RF, RF, SVM and GBDT. DeepNSI was able to predict the presence of elements, apart from carbon, which is ubiquitous anyway, in molecules of interest based on their photo-neutron spectra. In addition, DeepNSI showed very good sensitivity and was able to detect elements such as nitrogen with an atomic fraction below 4%. It can certainly be refined to improve the performances based on more training data. Thanks to its modularity, adding models to detect other elements like phosphorus or fluorine through their neutron signatures is also an option as they can also be found in some chemical weapons. The method proposed is therefore a promising option for element identification based on photo-neutron spectrometry.

This universal and portable structure allows to consider many other applications for DeepNSI, such as the detection of light elements for applications other than illicit material detection or for neutron sources identification in the context of radiation protection and decommissioning with mixed neutron spectra.

ACKNOWLEDGMENTS

This research benefited from a grant from the French National Laboratory of Metrology and Testing. The authors gratefully acknowledge Mr Quentin Besnard for discussions and numerous suggested improvements.

REFERENCES

1. Y. Zhao, T. Cui, Y. Yang, "The design of a photo-neutron source for the narcotic drugs detection in a large-truck". *Proceedings of 2017 IEEE Nuclear Science Symposium and Medical Imaging Conference (NSS/MIC 2017)*, Atlanta, Georgia, October 21–28 (2017).
2. C. Lino Fontana et al., "Detection system of the first rapidly relocatable tagged neutron inspection system (RRTNIS), developed in the framework of the European H2020 C-Bord project", *Physics Procedia*, **90,** pp. 279-284 (2017).
3. M. Gmar et al., "Detection of nuclear material by photon activation inside cargo containers", *Proceedings of SPIE Defense and Security Symposium*, Orlando, Florida, April 17–21 (2006).
4. K.W. Habiger, et al., "Explosives detection with energetic photons", *Nuclear Instruments and Methods in Physics Research Section B: Beam Interactions with Materials and Atoms*, **56-57**(2), pp. 834-838 (1991).
5. X. Fan, et al., "Deep learning-based component identification for the Raman spectra of mixtures", Analyst, **144**(5), pp. 1789-1798 (2019).
6. H.-T. Zeng, et al., "Mixture analysis using non-negative elastic net for Raman spectroscopy", *Journal of Chemometrics*, **3** (2020).
7. LeCun et al., "Handwritten digit recognition with a backpropagation network", *Advances in neural information processing systems*, pp. 396-404 (1990).
8. C. Ahdida et al., "New Capabilities of the FLUKA Multi-Purpose Code", *Frontiers in Physics,* 9 788253 (2022).
9. S. Agostinelli et al., "Geant4—a simulation toolkit", *Nuclear Instruments and Methods in Physics Research Section A: Accelerators, Spectrometers, Detectors and Associated Equipment*, **506**(3), pp. 250–303, (2003).
10. C. J. Werner, "MCNP users manual - code version 6.2", *LA-UR-17-29981*, (2017).
11. T. Sato et al., "Features of particle and heavy ion 435 transport code system (PHITS) version 3.02", *Journal of Nuclear Science and Technology,* **55**(6), pp. 684–690, (2018).
12. M. C. White et al., "Photonuclear physics in MCNP(X)", *Nuclear Applications of Accelerator Technology*, LA-UR99-4827, Long Beach, California, (1999).
13. M. C. White, "Release of the la150u photonuclear data library", *X-5:MCW-00-87(U)*, Los Alamos National Laboratory, (2000).
14. D. Kingman, J. Ba, "Adam: A Method for Stochastic Optimization", *Proceedings of the 3rd International Conference for Learning Representations*, San Diego, California, May 7–9 (2015).

APPENDIX A

DeepNSI flowchart. The neutron spectra for 18 MV and 20 MV photon irradiations of each pure compound in the database are used for data augmentation, and both positive and negative samples are generated with equal size. The augmented dataset of each compound is divided into three parts respectively for training, validation and testing. The 11 one-element identification models (noted M in the flowchart) are trained and saved for further prediction.

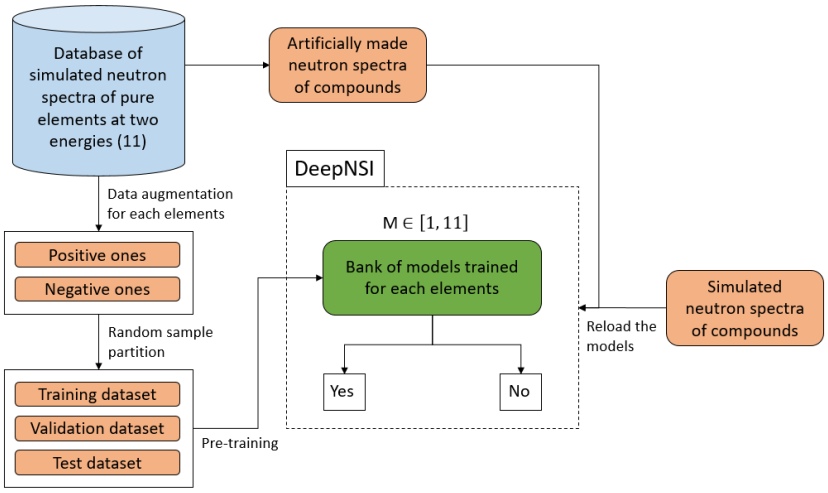

APPENDIX B

Confusion matrix between true elements and predicted elements for 1000 spectra of 3-element compounds randomly picked from the database and generated with random ratios in [0.0. 1.0] and a random noise of 1% of each spectrum's maximum.